

Catalytic Efficiency of Gold (III) and Gold Nanoparticles on the Oxidation of N-Pentane to N-Decane by *In Situ* Generated Sodium Ferrate under Microwave Irradiation

Manish Srivastava* and Anamika Srivastava

Department of Chemistry, BanasthaliVidyapith, Banasthali, Rajasthan, 304022, India.

Received: 21 Oct. 2016, Revised: 25 Nov. 2016, Accepted: 30 Nov. 2016.

Published online: 1 Jan. 2017.

Abstract: Oxidation of aliphatic hydrocarbons by *in situ* generated sodium ferrate in acid medium catalyzed by gold (III) and gold nanoparticles under microwave irradiation. In following analysis used the citrate reduction and green methodology process for the synthesis of gold nanoparticles. The size of gold nanoparticles was found that the average particle size of individual gold nanoparticles is approximately 20-50nm. Aliphatic hydrocarbons converted to the aliphatic acids by oxidation reaction. In case of gold nanoparticles gives the higher yield as compare to gold (III) catalyst because in the presence of nanoparticles the yield become higher as compared to catalyst in solution phase because in nanoparticles size is decreased (in nm) so surface area become increase so catalytic activity increase many times as compared to catalyst in solution phase.

Keywords: Oxidation, Aliphatic Hydrocarbons, Gold nanoparticles, Gold(III) Solution, *In situ* generated Sodium Ferrate, Microwave Irradiation.

1 Introduction

The catalytic oxidation of aliphatic, aromatic hydrocarbons and alcohols in the presence of transition metal has been of contemporary interest due to diversified potentials in organic chemistry and industrial manufacturing, and is recognized a fundamental reaction.[1-4]

Nanocatalysis is an interdisciplinary research field involving chemistry, engineering, biology, and medicine and has great potential for early detection, accurate diagnosis, and personalized treatment. Transition metals make good catalysts. The shape-controlled synthesis of metal nanoparticles has been an extremely active research area in recent years owing to their fascinating shape-dependent optical, electronic, and catalytic properties [5-9].

In liquid phase catalytic oxidation of benzyl alcohol to benzaldehyde over vanadium phosphate catalyst[10] The most common metals used for catalysis are Pd, Pt, Au, Ag, Fe, and Cu. Thus, optimizing the usage of active materials has been a major aspect of catalyst optimization and thus many scientists have studied catalysis by nanoparticles in order to take advantage of the higher surface areas exposed to the reactants.[11-12]

Catalytic properties of nanoparticles as catalysts increased as nanoparticles properties and reactions were better understood. The possibility of using less material and

having diverse properties for different shapes of nanoparticles is very attractive. Bulk gold, being the most stable among all metals, was for many years considered as an inert catalyst. However, gold particles with size on the scale of nanometers (Au NPs) have been recognized as surprisingly active and extraordinary effective green catalysts, generating a highly popular research topic in the frontier between homogeneous and heterogeneous catalysis [13].

The novel work of Haruta et al. [14] discovered that gold was the preeminent catalyst for CO oxidation. Hutchings¹⁵ explained gold to be the excellent catalyst of choice for acetylene hydro chlorination, and showed that supported nano gold catalysts have found a broad range of applications in selective chemical transformations¹⁶ with respect to alcoholic oxidation. Many researchers have reported the use of highly active metal catalysts for the oxidation of alcohols.

Baatz et al. [17] reported on the use of gold catalysts in the liquid-phase oxidation of glucose to gluconic acid. Use of gold can be more selective than platinum and palladium for this reaction. [18] In further, focus is on the use of gold nanoparticles as a catalyst for the oxidation of alcohols. [19]

Iron commonly exists in the +2 and +3 oxidation states; however, in a strong oxidizing environment, higher oxidation states of iron such as +4, +5 and +6 can also be

* Corresponding author E-mail: sagermanish1@gmail.com

obtained [20]. Fe (VI) is a powerful oxidizing agent throughout the entire pH range with a reduction potential (Fe (VI)/Fe (III) couple) varying from +2.2 V to +0.7 V versus NHE in acidic and basic medium. Sodium ferrate oxidizes alcohols to aldehydes or ketones [21]. Sodium ferrate oxidizes the aromatic hydrocarbons to corresponding carbonyl compounds and cyclic alcohols and aldehydes converted to aldehydes and acids. [22]

In aqueous solution, the ferrate dianion FeO_4^{2-} remains monomeric²³ in basic solution the rate of decomposition of ferrate is highly variable. pH and temperature are the key factors, but light does not affect the stability of ferrate solutions.²⁴ In dilute solution, the lowest rate of reduction of ferrate by water occurs between pH 9.4 and 9.7.[25] In strong alkali (3M or above), ferrate solutions reach another region of stability, thus allowing the preparation and purification of potassium ferrate by wet method. [26-27] the main problem with sodium or potassium ferrate is their separation, which requires tedious processes. Sodium ferrate (Na_2FeO_4) has received much attention because of its utility in green organic synthesis and waste water treatment processes [28-29].

2 Experimental Section

2.1 Synthesis of Gold nanoparticles

Gold nanoparticles were synthesized by using a well-documented citric acid route (Turkevich, et al., 1951; Frens, 1973 method). 5.0 ml of 0.05 M trisodium citrate was added to 10 ml of 2.55×10^{-3} M boiling chloroauric acid aqueous solution while stirring. The mixture was kept boiling for about 30 min until a wine red color was observed, indicating the formation of gold nanoparticles and then cool down at room temperature. Gold nanoparticles were isolated from the colloidal solution by centrifugation at 15000 RPM for 30 min and then washed 3-4 times with de-ionized water. The fast stirring of solution is responsible for formation of uniform gold nanoparticles. Gold nanoparticles have some negative surface charges due to the adsorption of anions, Cl^- or citrate, and they were not aggregated.

2.2 Oxidation of aliphatic hydrocarbons

N-pentane, n-hexane, n-heptane and n-decane were used as such without further purification. In a typical procedure, sodium ferrate was prepared by taking ferric nitrate ($\text{Fe}(\text{NO}_3)_3 \cdot 9\text{H}_2\text{O}$) 4.49 mmol in a 50 ml flask and the required amount 44.7 – 58.8 mmol of sodium hypochlorite solution was added drop-wise with constant stirring. Formation of a clear dark purple-red colored solution indicates the formation of ferrate dianions. Solution of gold (III) chloride was prepared by dissolving the sample Hydrochloroauric acid trihydrate (III) in de-ionized water the final strength of catalyst is 2.55×10^{-3} mmol.

A CEM Discover Microwave synthesizer was used for studying the reactions under microwave irradiation, in which control of temperature, time and power was possible. In order to achieve the maximum yield, three to six sets were performed by changing the concentration, time, temperature and other reaction conditions of each component, which can affect the yield of product for example in the synthesis of pentanoic acid from n-pentane for performing the reactions in the solution phase, 0.63×10^{-3} mmol of gold(III) chloride with 4.49 mmol ferric nitrate and 44.1 mmol sodium hypochlorite added to 3.4 mmol of acetic acid solution containing 1.0 mmol of n-pentane and the mixture was heated under microwave irradiation for 3.0 min taken in a microwave vessel. Contents were cooled and extracted with diethyl ether. The extract was dried over anhydrous MgSO_4 . Replacing the gold solution in above reaction mixture with the gold nanoparticles was heated under microwave irradiation for 3.0 min. Contents were cooled and extracted with diethyl ether the extract was dried over anhydrous MgSO_4 and prepared the amide derivative of the product and noted the achieved yield. IR (Bruker 8201 IR spectrophotometer) and ^1H NMR (Bruker 400MHz) spectra were recorded.

3 Results and Discussion

3.1 Characterization of gold nanoparticles

3.1.1 UV spectral analysis

UV-Vis spectroscopy is an effective method to show the evolution of metallic species during the formation of colloidal gold nanoparticles. As shown in Fig 1 the optical absorbance plasmon band of the gold nanoparticles in the colloidal suspension is about 520 nm. This peak arises due to absorption of energy, which is caused by collective oscillations of the conduction electrons upon excitation with visible light shows wine red color of gold nanoparticles. The surface plasmon bands are broad and the intensity increases indicating increase in production of nanoparticles.

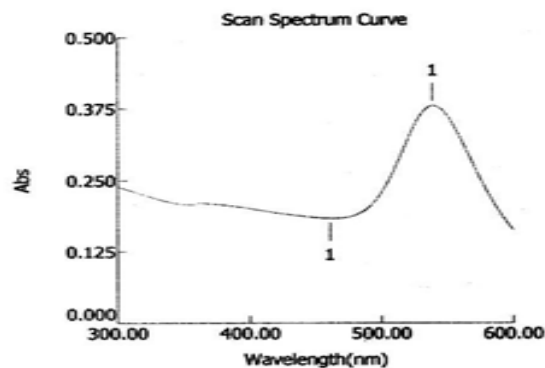


Fig 1 UV-Vis Spectrum of gold nanoparticles (Au NPs)

3.1.2 Zeta sizer and zeta potential measurement

Table1: XRD analysis of all the peaks of gold nanoparticles using 0.154 nm wavelength.

S. No	2 θ (degrees)	FWHM (degrees)	$\beta = \Pi * \text{FWHM} / 180$ (radians)	$D = k \lambda / \beta \cdot \text{Cos}\theta$ (nm)	Average Value D(nm)
Gold Nanoparticles	23.16	0.4125	0.0071	19.34	18.07
	34.97	0.5161	0.0090	16.12	
	43.01	0.6022	0.0105	14.19	
	55.15	0.3985	0.0069	22.66	

Table 2: Effect of diverse factors on the yield of pentanoic acid (Amide derivative) from pentane (1.0mmol) by gold (III)-Sodium ferrate catalytic system in aqueous acetic acid medium in solution phase under microwave irradiation

S. No.	Acetic acid $\times 10^2$ (mmol)	Fe (NO ₃) ₃ · 9H ₂ O (mmol)	NaClO (mmol)	Au(III) $\times 10^3$ catalyst (mmol)	Time (min)	Temp. (°C)	MW power (W)	% yield With Au(III) catalyst
1.	3.4	2.24	29.4	0.16	2.0	50	40	14.83
2.	3.4	4.49	44.1	0.48	2.0	60	80	40.53
3.	3.4	4.49	44.1	0.63	3.0	70	80	60.31
4.	3.4	5.61	51.4	0.63	3.3	90	120	34.10

Table 3: Comparative study of gold (III) chloride and gold nanoparticles as catalyst in solution phase for oxidation of aliphatic hydrocarbons by *in situ* generated sodium ferrate in acetic acid medium under microwave irradiation
a- In presence of Au (III) solution, b- In presence of gold nanoparticles(Au NPs)

Organic Substrate	Product	Acetic acid $\times 10^2$ (mmol)	Fe(NO ₃) ₃ + NaClO (mmol)	Time (min)	Temp (°C)	MP (reported) °C	MW Power (W)	% Yield With Au (III) catalyst ^a	% Yield With Au NPs ^b
Pentane (A)	Pentanoic acid(A')	3.4	4.49+ 44.1 ^a 4.49+ 44.1 ^b	3.0 ^a 3.0 ^b	70 ^a 70 ^b	104 (106)	80 ^a 80 ^b	60.31	65.14
Hexane (B)	Hexanoic acid (B')	3.4	5.61+ 44.1 ^a 5.61+ 44.1 ^b	2.3 ^a 2.3 ^b	70 ^a 70 ^b	100 (101)	80 ^a 80 ^b	60.77	65.34
Heptane (C)	Heptanoic acid (C')	3.4	5.61+ 51.4 ^a 5.61+ 51.4 ^b	2.0 ^a 2.0 ^b	90 ^a 90 ^b	94 (162)	100 ^a 100 ^b	71.91	78.05
Decane (D)	Decanoic acid (D')	3.4	4.49+ 51.4 ^a 4.49+ 51.4 ^b	3.0 ^a 3.0 ^b	100 ^a 100 ^b	90 (92)	100 ^a 100 ^b	76.04	79.68

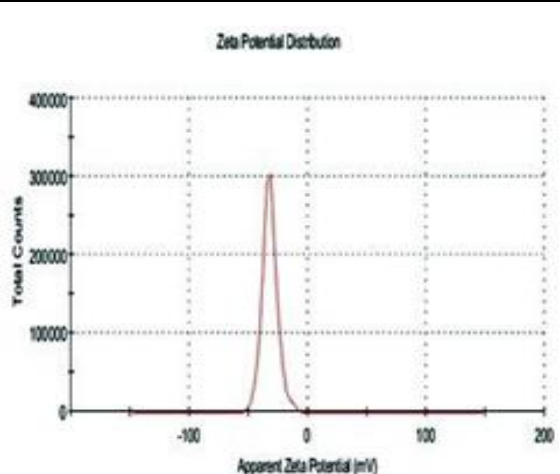


Fig 2(A) Zeta potential of Au NPs

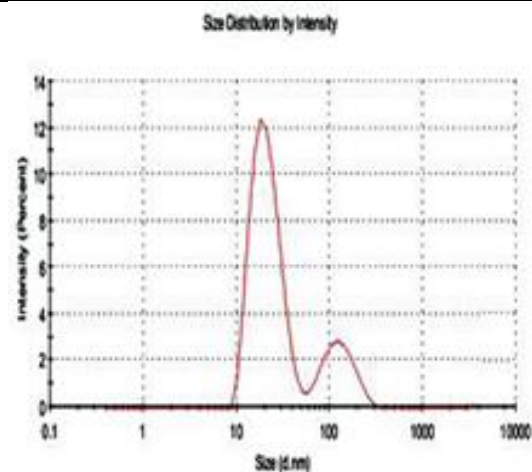


Figure 2(B) Zeta sizer of Au NPs

3.1.3 XRD analysis of gold nanoparticles

The dried mixture of gold nanoparticles was collected to determine the formation of gold nanoparticles by X-ray diffractometer operated at a voltage of 30 kV and a current of 30 mA with CuK α radiation in a θ -2 θ configuration. In addition, the strong sharp reflections indicate that relatively large particles feature in the support, whereas the broad reflections mean the gold size is relatively small. The XRD pattern of prepared gold nanoparticles in the 2 θ range 10° to 60° is shown in **Fig 3** Diffraction peaks corresponding to face centered cubic (fcc) structure of gold nanoparticles in a crystalline nature having sharp peaks at 23.16°, 34.97°, 43.01° and 55.15° are assigned to plane of (111), (200), (222) and (311). To calculate the average particle size, the full width half maxima data with help of Debye-Scherrer formula was used, which is given below.

$$D = 0.9\lambda / \beta \cos\theta$$

Where D is the particle size of the nanoparticles, ' λ ' wavelength of X-rays, ' β ' the broadening of diffraction line measured at half its maximum intensity in radians and ' θ ' Bragg's angle.

The average particle size of gold nanoparticles was found 18.07 nm by XRD methods.

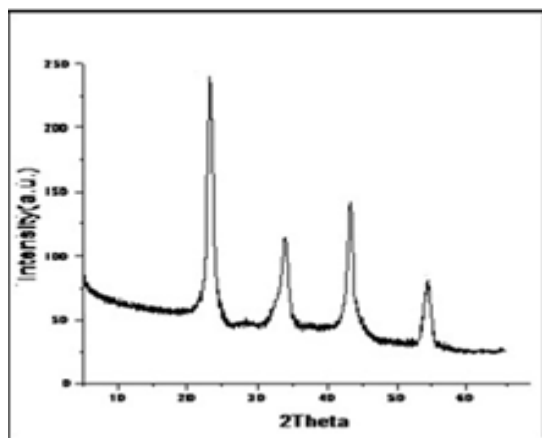


Fig 3 XRD of gold nanoparticles (Au NPs).

3.1.4 FESEM and TEM analysis of gold nanoparticles

Morphological analysis of colloidal gold particles by SEM and TEM methods revealed that the synthesized gold nanoparticles spherical in shape with smooth surface. Scanning electron micrograph of the synthesized nanoparticles is presented in **Figure 4(a)**. The SEM image shows that the average diameter of gold nanoparticles was found to be around 50nm. The TEM images showed in **Figure 4(b)** that most of the gold nanoparticles are round or spherical dark colored dot of colloidal gold with the average diameter of about 50nm. It is found that the average particle size of individual gold nano particles is

approximately **20-50nm** based on zeta seizer, XRD, SEM and TEM analysis.

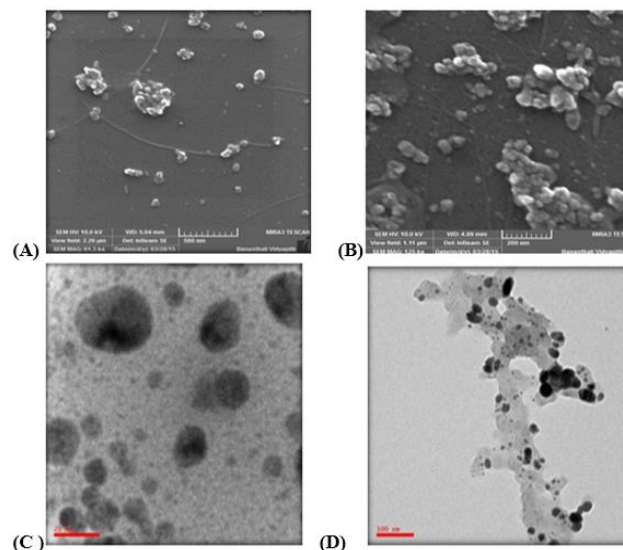


Fig 4 (a) FESEM image and 4(b) TEM image of gold nanoparticles (Au NPs).

3.2 Spectral analysis of organic compounds

Pentanoic acid: IR peaks: $\nu_{\max} = 3335.75 \text{ cm}^{-1}$ ($\nu_{\text{O-H}}$), 1278.89 cm^{-1} ($\nu_{\text{C-O str}}$), 1690.17 cm^{-1} ($\nu_{\text{C=O}}$).

NMR Signals: δ 11.1485 (1H, s), δ 2.1676- 2.2794 (2H, t), δ 1.2612-1.32591 (3H, t), δ 1.3451-2.1888 (4H, m).

Hexanoic acid: IR peaks: $\nu_{\max} = 3500.75 \text{ cm}^{-1}$ ($\nu_{\text{O-H}}$), 1248.89 cm^{-1} ($\nu_{\text{C-O str}}$), 1695 cm^{-1} ($\nu_{\text{C=O}}$).

NMR Signals: δ 11.1612 (1H, s), δ 2.2394- 2.4171 (2H, t) δ 1.1485-1.2627 (3H, t) δ 1.2859-2.2162 (6H, m).

Heptanoic acid: IR peaks: $\nu_{\max} = 3028.90 \text{ cm}^{-1}$ ($\nu_{\text{O-H}}$), 1248.05 cm^{-1} ($\nu_{\text{C-O str}}$), 1703.69 cm^{-1} ($\nu_{\text{C=O}}$).

NMR Signals: δ 11.1142 (1H, s), δ 2.2063 -2.2829 (2H, t) δ 0.9691-1.0796 (3H, t) δ 1.3379 - 1.9950 (8H, m).

Decanoic acid: IR peaks: $\nu_{\max} = 3335.75 \text{ cm}^{-1}$ ($\nu_{\text{O-H}}$), 1278.89 cm^{-1} ($\nu_{\text{C-O str}}$), 1689.10 cm^{-1} ($\nu_{\text{C=O}}$).

NMR Signals: δ 11.1135 (1H, s), δ 2.2729 -2.2379 (2H, t) δ 0.9319-1.0511 (3H, t) δ 1.2345 - 1.9985 (14H, m).

4. Discussion

In case of catalyst variation (entries 1, 2 and 3, Table 2) increase the concentration of catalyst decrease the yield of the product because at high concentration un- reactive species is formed so the yield of product is decrease. Yield reaches to a maximum and then starts decreasing with further increase in the amount of ferric nitrate (entries 2, 3 and 4, Table 2) while yield decreases with increasing amount of sodium hypochlorite (entries 2,3, and 4, Table

2). Probable reason for this appears to be the decomposition of ferrate ions. It is well known that the decomposition of high-valent oxy anions is catalyzed by traces of impurities like the reducing organic materials or metal traces, which may be present in these reactants

In Fig 5 the comparative bar diagram show that in the presence of gold nanoparticles the yield become higher as compared to gold ions in solution phase because in nanoparticles size is decreased (in nm) so surface area become increase so catalytic activity increase many times as compared to catalyst in solution phase.

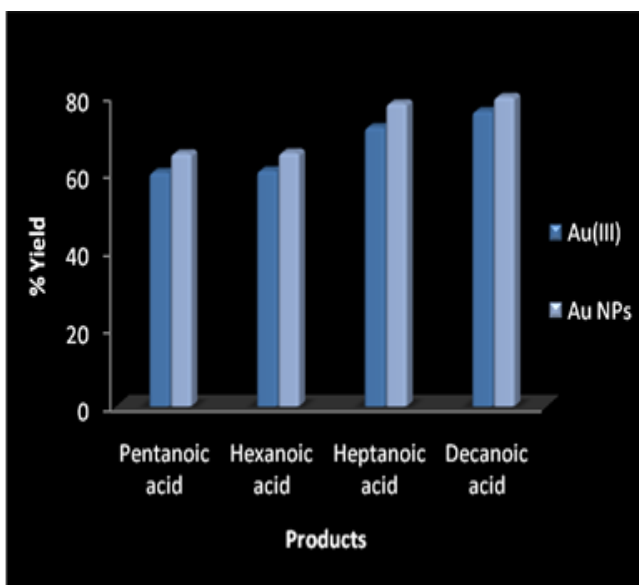


Fig 5 Comparative bar diagram of gold (III) chloride and gold nanoparticles on the yield of aliphatic acids.

5 Conclusions

The study was principally mostly to determine the effectiveness and economy of the narrative, straightforward, one-pot novel Au^{3+} -sodium ferrate and Au^0 -sodium ferrate. In conclusion, we have developed a rapid and efficient microwave assisted procedure for the synthesis of various organic compounds using new catalytic system and mentioned the yield comparison on using *in situ* generated sodium ferrate as oxidants. The reported novel one-pot system is highly competent, effortless, and can be used to oxidize a multiplicity of other functional groups, for which studies are being done. Microwave reactions are also important from the environmental point of view because using very less amount of solvent and not use the hazardous chemical in reaction.

Supplementary information (SI)

All additional information pertaining to characterization of the compounds, IR spectra (1 to 4) and NMR spectra (1 to

4) are given in the supporting information.

Acknowledgement

The authors are grateful thanks to help from Department of chemistry Banasthali University, Rajasthan, India and Punjab University is acknowledged for spectral studies.

References

- [1] Katritzky, R; Meth-Cohn, O; Rees, C. W; and. Pattenden, G; 1995, "Comprehensive Organic Functional Group Transformations: Reactions, Mechanisms, and Synthesis," Elsevier Science, Oxford.
- [2] Larock, R. C.; 1999, "In Comprehensive Organic Transformations: A Guide to Functional Group Preparations," 2nd Edition, Wiley-VCH, New York.
- [3] Smith, M. B.; and March, J.; 2001, "Advanced Organic Chemistry: Reactions, Mechanisms, and Structure," 5th Edition, Wiley-Interscience, New York.
- [4] Sheldon, R. A.; and Van Bekkum, H.; 2001, "Fine Chemicals through Heterogeneous Catalysis," Wiley-VCH Verlag GmbH & Co., Weinheim.
- [5] Feldheim, D. L.; Foss, C. A. Jr. 2002, "Metal Nanoparticles: Synthesis, Characterization and Applications". New York, Dekker
- [6] Burda, C.; Chen, X.; Narayanan, R.; El-Sayed, M. A. 2005, "Chemistry and properties of nanocrystals of different shapes" Chem Rev 105, 4, 102-1025.
- [7] Daniel, M. C.; Astruc, D. 2004, "Gold nanoparticles: assembly, supramolecular chemistry, quantum-size-related properties, and applications toward biology, catalysis, and nanotechnology". Chem. Rev. 104, 1, 293-346.
- [8] Murphy, C. J.; Sau, T. K.; Gole, A. M.; Orendorff, C. J.; Gao, J.; Gou, L.; Hunyadi, S. E.; Li, T. 2005, "Anisotropic metal nanoparticles: Synthesis, assembly, and optical applications". J. Phys. Chem. B, 109, 29, 13857-13870.
- [9] Liz-Marzan, L. M. 2006, "Tailoring surface plasmons through the morphology and assembly of metal nanoparticles". Langmuir, 22, 1, 32-41.
- [10] Behera, GC; Parida. K.M.; 2012, "Liquid phase catalytic oxidation of benzyl alcohol to benzaldehyde over vanadium phosphate catalyst"; Applied Catalysis A: General 413– 414, 245– 253.
- [11] Atkins, P.W.; Overton, T.L; Rourke, J.P; Weller, M.T.; Armstrong, F.A.; 2010, "Inorganic chemistry", New York: W. H. Freeman and Company, 5th Ed, 690-720.
- [12] Dash. P; 2010, "Towards the rational design of nanoparticles catalysts, PhD thesis" University of Saskatchewan, Saskatoon, Canada. 690-720.
- [13] Astruc, D.; Lu, F.; Aranzues, J. R. 2005, "Nanoparticles as Recyclable Catalysts: The Frontier between Homogeneous and Heterogeneous Catalysis" Angewandte Chemie., Int. Ed., 44, 7852-7872.
- [14] Haruta, M.; Yamada, N.; Kobayashi, T.; S. Iijima, 1989, "Gold catalysts prepared by coprecipitation for low-

- temperature oxidation of hydrogen and of carbon monoxide". *J. Catal.* 115, 301–309.
- [15] Hutchings, G. J. 1985, "Vapor phase hydro chlorination of acetylene: correlation of catalytic activity of supported metal chloride catalysts" *J. Catal.* 96, 292–295.
- [16] Hashmi, A.S.K.; Hutchings, G. J. 2006, "Gold catalysis" *Angew. Chem. Int. Ed.* 45, 7896–7936.
- [17] Baatz, C.; Prube, U.; 2007, "Preparation of gold catalysts for glucose oxidation by incipient wetness", *Journal of Catalysis.* 249, p.34–40.
- [18] L. M. Rossi; 1998, "Gold nanoparticle catalyzed oxidation of alcohols from biomass to commodity chemicals". *Journal of Catalysis.* 176, 552.
- [19] Abad, A.; Concepción, P.; 2005, "Gold nanoparticle catalyzed oxidation of alcohols from biomass to commodity chemicals", *Angew. Chem. Int. Ed.* 44, 4066 (b) Edwards, D.I.; 2006, "Gold nanoparticle catalyzed oxidation of alcohols from biomass to commodity chemicals Science", 311, 362.
- [20] Perfiliev, Y.D.; and Sharma, V.K.; 'Higher Oxidation States of Iron in Solid State: Synthesis and Their Mössbauer Characterization". *ACS Symposium Series*, 985, chapter 7, 112–123
- [21] Tandon, P.K.; Singh, S.B.; Srivastava, M; 2007, "Synthesis of some aromatic aldehydes and acid by sodium ferrate in the Presence of copper-nano particles absorbed on K10 Mont Morillonite using microwave irradiation". *Appl. Organometal. Chem.* 21, 264-267.
- [22] Tandon, P.K.; Singh, S.B.; Singh, S.; Kesarwani, B, 2012, "Oxidation of hydrocarbons, cyclic alcohols and aldehydes by in situ prepared sodium ferrate". *J.Indian Chem. Soc.* 89, 1363-1367.
- [23] Guff H, Murmann RK; 1971, "Mechanism of isotopic oxygen exchange and reduction of ferrate (VI) ion (FeO_4^{2-})", *J. Am. Chem. Soc.* 93, 6058-6065.
- [24] Wagner WF, Gump JR, Hart EN; 1952, "Factors Affecting Stability of Aqueous Potassium Ferrate (VI) Solutions". *Anal. Chem.*, 24, 1497- 1498.
- [25] Lee DG, Gai H; "Kinetics and mechanism of the oxidation of alcohols by ferrate ions". 1993, *Can. J. Chem.* 71, 1394-1400.
- [26] Schreyer. JM, Thompson. GW, Ockermann LT; 1951, "Preparation and Purification of potassium ferrate. VI". *J. Am. Chem. Soc.*, 73, 1379–1381.
- [27] Maghraoui. A.El; Zerouale. A; Ijjaali. M', Sajieddin. M; 2012, "Synthesis and Characterization of Ferrate (VI) Alkali Metal by Wet method" *International Journal of Modern Engineering Research*, 2, 6, 4521-4523.
- [28] Tandon. P.K.; Singh. S.B.; Shukla. R.C.; 2013, "Antimicrobial and Oxidative Properties of Sodium Ferrate for the Combined Removal of Arsenic in Drinking Water with Shell Ash of Unio". *Industrial & Engineering Chemistry Research* 52 (48), 17038-17046.
- [29] Tandon. P.K.; Singh. S.B.; 2011, "Hexacyanoferrate (III) oxidation of arsenic and its subsequent removal from the spent reaction mixture", *Journal of hazardous materials* 185 (2), 930-937.
-